Available online at www.sciencedirect.com

SciVerse ScienceDirect

Ceramics International 38 (2012) 2785–2791

CERAMICS INTERNATIONAL

www.elsevier.com/locate/ceramint

Microstructure and electrical properties of Mn/Y codoped $Ba_{0.67}Sr_{0.33}TiO_3$ ceramics

Dongxu Yan [a,b], Zunping Xu [a], Xiaolong Chen [a], Dingquan Xiao [a], Ping Yu [a], Jianguo Zhu [a,*]

[a] College of Materials Science and Engineering, Sichuan University, Chengdu 610064, PR China
[b] China Academy of Engineering Physics, P.O. Box 919-71, Mianyang 621907, PR China

Received 14 November 2011; received in revised form 20 November 2011; accepted 20 November 2011
Available online 28 November 2011

Abstract

Pure and Mn/Y codoped $Ba_{0.67}Sr_{0.33}TiO_3$ (BST) ceramics were fabricated via the citrate–nitrate combustion technique, and the microstructure and electrical properties of BST ceramics were mainly investigated. The Mn/Y codoping concentration has a strong influence on the microstructure and electrical properties of BST ceramics. All BST ceramics possess a pure polycrystalline structure. The density, dielectric loss, leakage current, and ferroelectric properties are improved by codoping 0.5 mol% Mn and 1.0 mol% Y to BST. The relative density of 0.5 mol% Mn/1.0 mol% Y-codoped BST (BST0510) ceramics reaches 97.5% of the theoretical value. BST0510 ceramics have the lowest dielectric loss ($\tan\delta < 0.0073$ at 1 kHz) among all BST ceramics. BST0510 ceramics also demonstrate a low leakage current density (1.23×10^{-7} A/cm^2) at an applied field of 10 kV/cm, and excellent ferroelectric properties with a remanent polarization of $2P_r = 15.327$ μC/cm^2 and a coercive field of $2E_c = 3.456$ kV/cm. Therefore, the Mn and Y with optimum content help improve the electrical properties of BST materials.

Keywords: C. Dielectric properties; BST; Ceramics; Ion substitution; Codoping

1. Introduction

In recent years, much attention has been given to the development of pyroelectric materials for heat–electric conversion in infrared detector and thermal imaging [1–4]. $Ba_{1-x}Sr_xTiO_3$ ceramics have been considered as a promising candidate for such applications due to a noticeable change in the dielectric constant with a paraelectric-to-ferroelectric phase transition taking place, which allows a large pyroelectric coefficient to be obtained near the vicinity of the phase transformation temperature [5]. And the temperature at which the material displays its largest temperature sensitivity can be matched exactly to devices' ambient temperature simply by changing Ba/Sr ratio [6], which enables such devices for use close at room temperature. The major challenge in designing material systems for pyroelectric devices is the simultaneous requirement of a high pyroelectric coefficient, a low heat capacity, and low dielectric constant and loss [7]. We have recently shown that $Ba_{0.67}Sr_{0.33}TiO_3$ ceramics have a pyroelectric coefficient of ~263 nC/(cm^2 K) with a dielectric loss of ~0.047 at 1 kHz [8]. Unfortunately, the dielectric loss of pure BST is high. In order to dilute the dielectric constant and reduce the dielectric loss, Mn has been introduced into BST, but the leakage current of BST ceramics increases.

The Y element has been identified as one of the ''magic dopants'' [9], improving the resistance degradation and reducing the leakage current. For example, Y-doped BST capacitors exhibit a tenfold lower leakage current density (10^{-9} A/cm^2 at 100 kV/cm) and 70% higher dielectric constant than those of nominally undoped BST-based capacitors [10]. Therefore, the introduction of Mn combined with Y presents an intriguing opportunity to develop BST materials for pyroelectric device applications with stringent demands focused on low dielectric loss and leakage current, while still maintaining a moderate pyroelectric coefficient. In this work, we present an experimental study on the effects of Mn and Y additions on the bulk density, microstructure, and electrical properties of BST ceramics, confirming that the Mn and Y codoping is an effective way to optimize the electrical properties of BST ceramics.

* Corresponding author. Tel.: +86 28 85412415; fax: +86 28 85416050.
E-mail addresses: nic0400@scu.edu.cn, joyner68@sina.com (J. Zhu).

0272-8842/$36.00
doi:10.1016/j.ceramint.2011.11.049

2. Experimental procedure

The citrate–nitrate combustion (CNC) method was used to prepare these powders following the composition of $Ba_{0.67}Sr_{0.33}TiO_3$ and $Ba_{0.67}Sr_{0.33}TiO_3$ codoped with 0.5 mol% for Mn and 0.6–1.2 mol% for Y dopants. Required amounts of barium nitrate, strontium nitrate, tetrabutyl-titanate solution and additions were dissolved in citrate solution to prepare the precursor solutions with the desired stoichiometry for the BST ceramics, which Manganese acetate and yttrium oxide were used as a source of Mn and Y, and glacial acetic acid and glycol were used as the solvents of tetrabutyl-titanate. The pH value of the solution was adjusted to 6–7 with ammonia water in order to the ionization of citrate. Then the precursor solution was placed in a furnace and dried at 150 °C for 24 h to dehydrate, condense, promote polymerization, break organic bonds and transform into soft and porous black powders. Finally, the powders were calcined at 900 °C for 3 h to synthesize the BST powders, and the BST powders obtained were crushed to fine powders, pressed uniaxially into pellets, and sintered into ceramics at 1250 °C.

The crystal structure and surface morphology of BST ceramics were determined via X-ray diffraction (XRD) and scanning electron microscope (SEM). The temperature dependence of dielectric properties was determined using a temperature measurement apparatus and a temperature control box attached to an Agilent E4980A LCR meter. The polarization electric-field (*P-E*) hysteresis loops and the leakage currents were measured using Radiant Precision Ferroelectric Measurement System (RT2000 Tester, USA).

3. Results and discussion

In this work, the Archimedean method was used for bulk density measurements of all ceramics. Relative densities were calculated as percentages of measured density compared to theoretical density. The bulk and relative densities of BST ceramics for different Y concentration are shown in Fig. 1. The bulk density value of ~5.51 g/cm^3 for undoped BST ceramics is in agreement with reported results [11,12]. The density of codoped BST ceramics, firstly increases from ~5.46 g/cm^3 to ~5.47 g/cm^3, reaches a maximum value of ~5.60 g/cm^3 with increasing the amount of Y from 0.6 to 1.0 mol%, and then decreases to 5.32 g/cm^3 with further increasing Y content. As a result, the optimum Y (1.0 mol%) addition helps to enhance the density of BST ceramics.

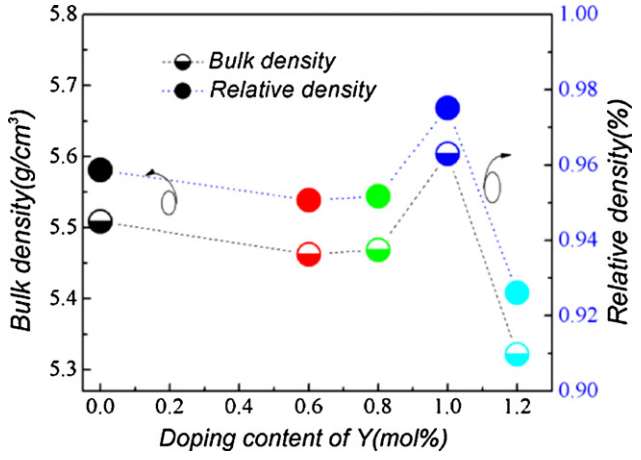

Fig. 1. Bulk and relative density of these BST ceramics.

Fig. 2A plots the XRD patterns of all ceramics. These XRD patterns reveal that all ceramics are a pure polycrystalline perovskite structure, indicating that the additions of Mn and Y are dissolved in the BST perovskite lattice. For further discussion, expanded XRD patterns are used to investigate the influence of Mn/Y codoping on the structure of BST ceramics, as shown in Fig. 2B. The (1 1 0) peak of codoped BST ceramics is firstly shifted to a higher angle with the increase of Y concentrations from 0.6 to 0.8 mol%, and then almost keeps unchanged with increasing Y from 1.0 to 1.2 mol%. This could

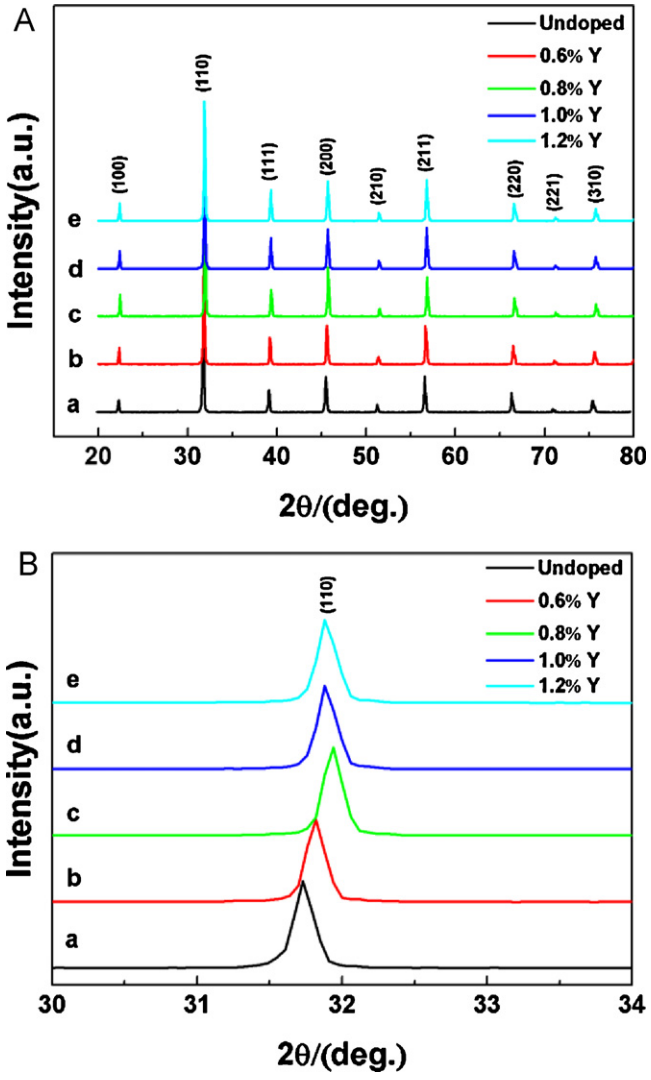

Fig. 2. XRD patterns of undoped and codoped BST ceramics (A), and expanded XRD patterns for the (1 1 0) peaks (B): (a) undoped, (b) 0.5 mol% Mn/0.6 mol% Y-codoped, (c) 0.5 mol% Mn/0.8 mol% Y-codoped, (d) 0.5 mol% Mn/1.0 mol% Y-codoped, and (e) 0.5 mol% Mn/1.2 mol% Y-codoped BST ceramics.

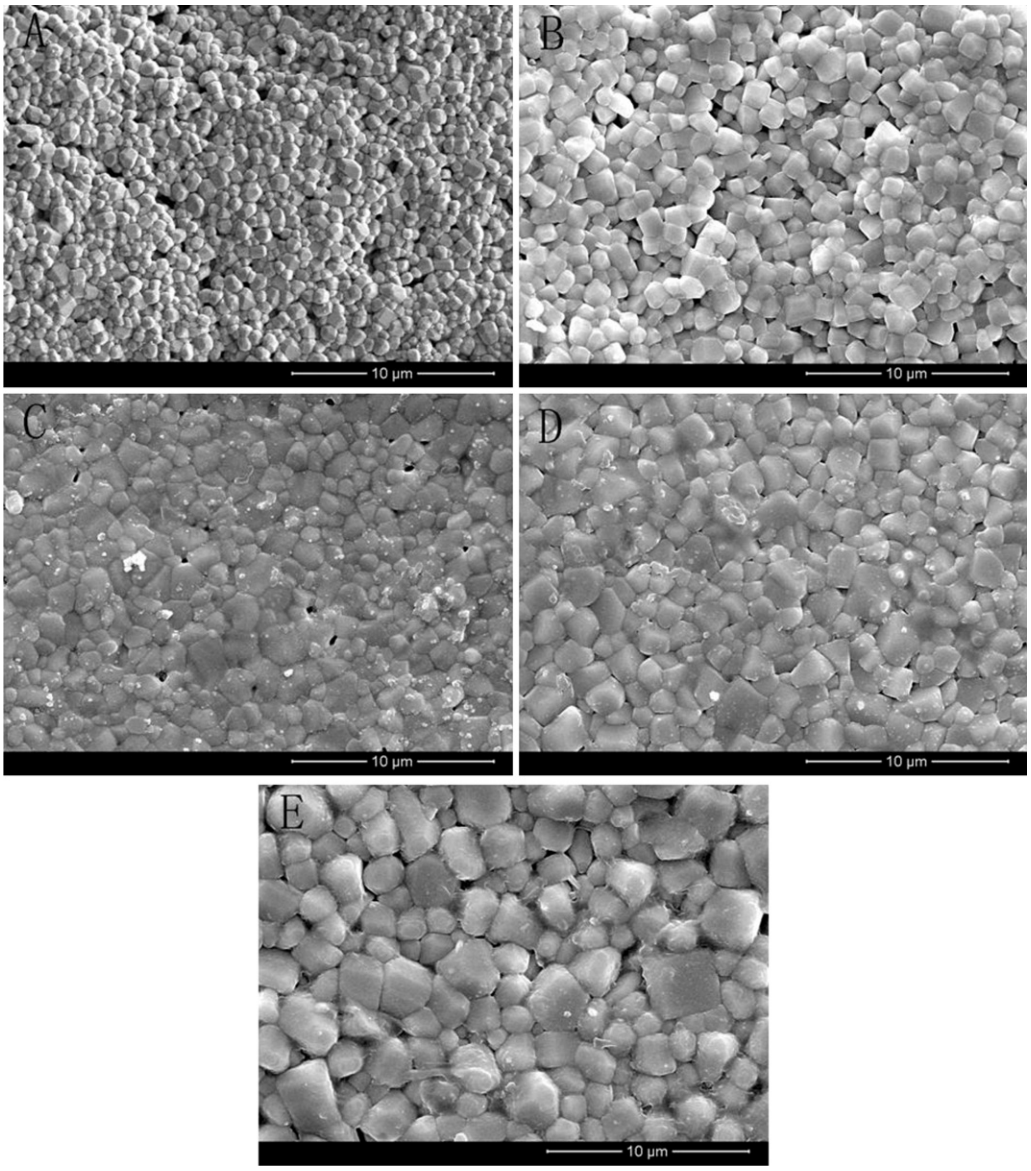

Fig. 3. SEM images of undoped and codoped BST ceramics: (A) undoped, (B) 0.5 mol% Mn/0.6 mol% Y-codoped, (C) 0.5 mol% Mn/0.8 mol% Y-codoped, (D) 0.5 mol% Mn/1.0 mol% Y-codoped, and (E) 0.5 mol% Mn/1.2 mol% Y-codoped BST ceramics.

be attributed to the substitution of $Mn^{2+}$and Y^{3+} ions to A site and/or B site ions in ABO_3, where ionic radiuses of Mn^{2+}, Y^{3+}, Ba^{2+}, Sr^{2+} and Ti^{4+} are 0.66 Å, 0.93 Å, 1.61 Å, 1.44 Å, and 0.61 Å, respectively. When the Y^{3+} concentration increases from 0.6 to 0.8 mol%, Y^{3+} and Mn^{2+} ions mainly substitute A site (Ba^{2+}, Sr^{2+}) ions and B site (Ti^{4+}) ions, respectively, leading to the shifting of the (1 1 0) peak to a higher angle, i.e. a decrease in lattice spacing. However, Y^{3+}ions substitute both A site ions and B ions in the BST structure when Y^{3+} concentration increases from 1.0 to 1.2 mol%, causing the perovskite lattice to slightly expand [10,13].

The effects of Mn and Y codopants on the microstructure of BST ceramics are shown in Fig. 3. The average grain size of undoped BST ceramics is ∼750 nm, while the grain size of codoped BST ceramics with Y concentration from 0.6 to 1.2 mol% is ∼1.4 μm, ∼1.6 μm, ∼2.1 μm, and ∼2.3 μm according to the SEM analysis, respectively. As shown in these SEM images, the undoped BST ceramics have small grains connected with each other and an extremely small amount of voids, while codoped BST ceramics have larger grains. The grain size of codoped BST ceramics becomes larger and more closed packed structure with increasing Y content. We believe that the introduction of these Mn and Y additions to $Ba_{0.67}Sr_{0.33}TiO_3$ decreases the sintering activation energy, lowers the sintering temperature of $Ba_{0.67}Sr_{0.33}TiO_3$, and thus leads to this closed packed structure.

The temperature dependence of dielectric constant (ε_r) and dielectric loss ($\tan\delta$) of BST ceramics at 1 kHz frequency are shown in Fig. 4A and B, respectively. It is noticeable that the dielectric constant peak does not decrease when the codoping content is 0.5 mol% Mn and 1.0 mol% Y. BST has been widely used as a dielectric bolometer [14–19], and its pyroelectric

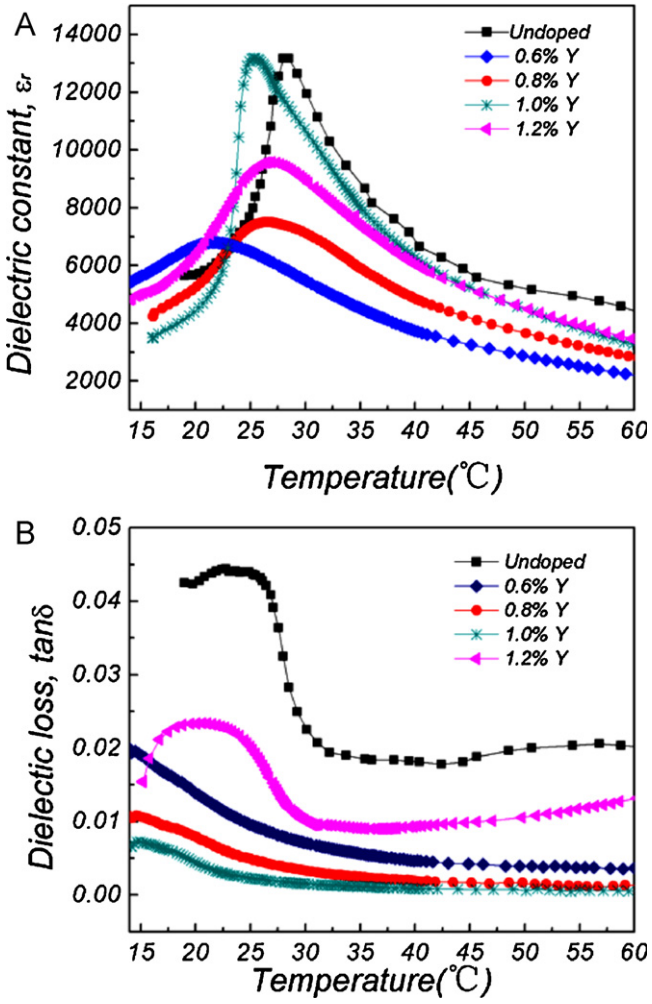

Fig. 4. Temperature dependence of dielectric constant (A) and dielectric loss (B) of undoped and codoped BST ceramics around T_c at 1 kHz.

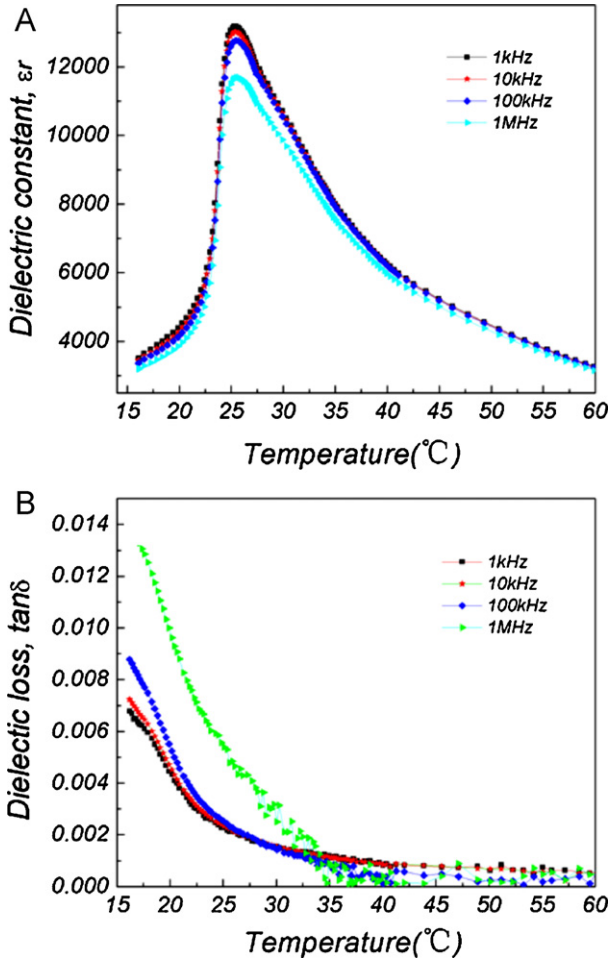

Fig. 5. Temperature dependence of dielectric constant (A) and dielectric loss (B) of 0.5 mol% Mn/1.0 mol% Y-codoped BST ceramics around T_c at 1 kHz, 10 kHz, 100 kHz, and 1 MHz.

coefficient can be obtained as follows:

$$p = \varepsilon_0 \int_0^E \left(\frac{\partial \varepsilon}{\partial T}\right) dE \approx \varepsilon_0 \left(\frac{\partial \varepsilon_r}{\partial T}\right) E \quad (1)$$

The steep dielectric constant peak indicates that $\partial\varepsilon_r/\partial T$ in Eq. (1) do not decrease when the Y doping content is 1.0 mol%, which is good for a pyroelectric application. The Mn/Y codoping decreases the dielectric loss of BST ceramics drastically, and the dielectric loss ($\tan\delta < 0.0073$ at 1 kHz) of BST0510 ceramics is the lowest among all BST ceramics.

Fig. 5A and B shows the temperature dependence of dielectric constant and dielectric loss of BST0510 ceramics with different frequencies, respectively. The dielectric constant slightly decreases with the increase of measurement frequencies. The dielectric constant peak of the ceramics is ~25.3 °C in these ε_r–T curves, corresponding to a paraelectric-to-ferroelectric phase transition. As the frequency increases, near the vicinity of the phase transformation temperature, the dielectric loss increases in the mass.

Fig. 6. displays the *P-E* hysteresis loops for these BST ceramics with various Y doping content, measured at 10 Hz and room temperature. Undoped BST ceramics show a ferroelectric hysteresis loop with a remanent polarization ($2P_r$) of 2.223 μC/cm^2 (Table 1.) and a coercive field ($2E_c$) of 0.964 kV/cm at an applied electric field of 50 kV/cm. These BST ceramics exhibit better hysteresis loops with increasing Y content from 0.6 to 1.0 mol%. $2P_r$ and $2E_c$ values of the 1.0 mol% Y-codoped BST ceramics are found to be 15.327 μC/cm^2 and 3.456 kV/cm, respectively. In this work, the Y substitution and a large grain size have contributed to the enhancement in the ferroelectric properties of the BST ceramics. However, 1.2 mol% Y-codoped BST ceramics show a distorted hysteresis loop, which may be induced by the factors of the large leakage current and low bulk density.

Improved ferroelectric properties of BST ceramics with increasing Y content could be explained by two reasons. The increased grain size of BST ceramics could contribute to the improved ferroelectric behavior of BST ceramics since the volume of dielectric polarization is proportional to the size of the grain. Moreover, the defect concentration also plays an important role on the ferroelectric behavior of BST ceramics in this work. For B-site occupancy, Mn and Y are acceptor-type dopants and the incorporation of Y^{3+} and Mn^{2+} to Ti^{4+} sites can

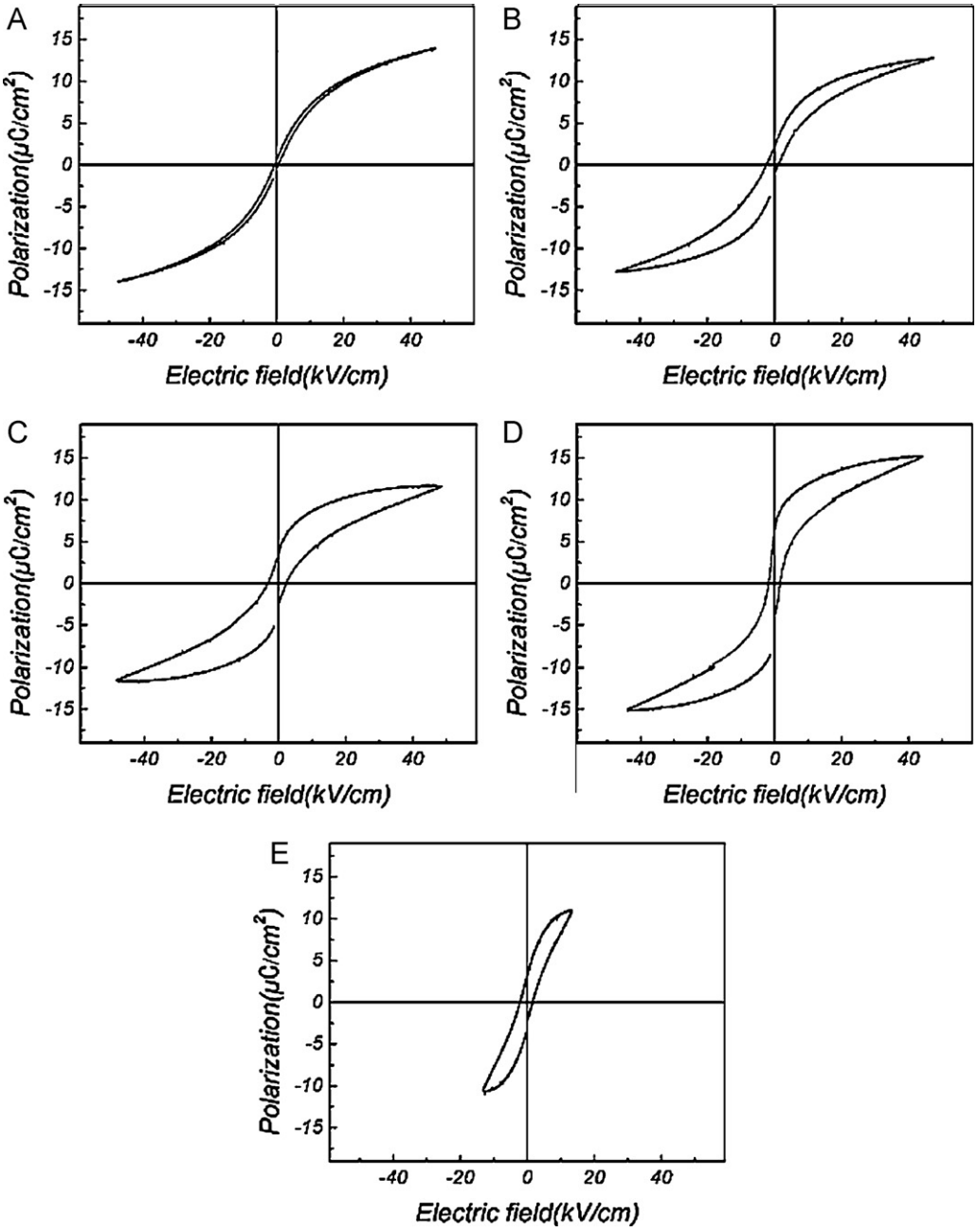

Fig. 6. *P-E* hysteresis loops at 10 Hz of undoped and codoped BST ceramics: (A) undoped, (B) 0.5 mol% Mn/0.6 mol% Y-codoped, (C) 0.5 mol% Mn/0.8 mol% Y-codoped, (D) 0.5 mol% Mn/1.0 mol% Y-codoped, and (E) 0.5 mol% Mn/1.2 mol% Y-codoped BST ceramics.

be expressed by the following point defect reactions.

$$Y_2O_3 + 2AO \xrightarrow{ABO_3} 2Y_B^{'} + 2A_A + 5O_O + V_O^{\bullet\bullet}$$

$$MnO + AO \xrightarrow{ABO_3} Mn_B^{''} + A_A + 2O_O + V_O^{\bullet\bullet}$$

When $Y^{3+}$and Mn^{2+} ions substitute Ti^{4+} in the BST lattice, oxygen vacancies ($V_O^{\bullet\bullet}$) are created in order to maintain the charge balance. Defect dipoles of $Y^{3+} - V_O^{\bullet\bullet}$ (or $Mn^{2+} - V_O^{\bullet\bullet}$) complexes could exist in the unit cells by binding Y^{3+} ions and oxygen vacancies. Defect dipoles are along the direction of the

Table 1
Ferroelectric parameters of undoped and Mn/Y-codoped BST ceramics.

Parameters	Undoped BST	0.5% Mn/0.6% Y	0.5% Mn/0.8% Y	0.5% Mn/1.0% Y	0.5% Mn/1.2% Y
P_r (μC/cm^2)	2.223	6.120	8.900	15.327	6.972
E_c (kV/cm)	0.964	3.513	5.527	3.456	3.645

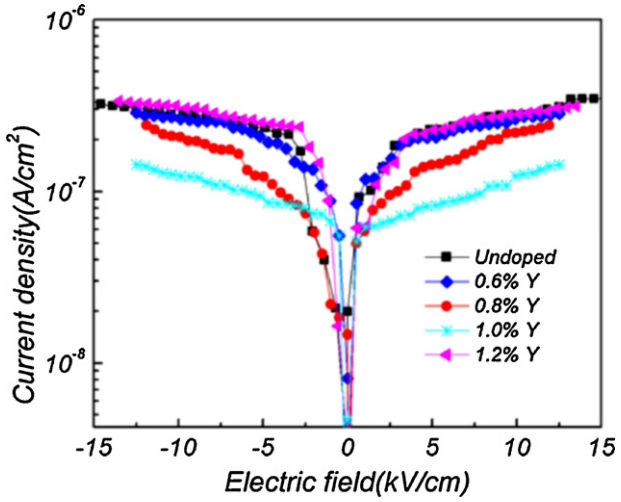

Fig. 7. The influence of codoping on the leakage current of BST ceramics at 25 °C.

spontaneous polarization in these BST materials. So the increase in the defect dipoles helps to improve the total polarizability.

Fig. 7 illustrates the leakage current characteristics of undoped and Mn/Y-codoped BST ceramics, measured at room temperature. The leakage current densities of BST ceramics decrease with increasing Y content from 0 to 1.0 mol%, and then increase with further addition of Y content. The leakage current density of the BST0510 ceramics is 1.23×10^{-7} A/cm^2 at an applied field of 10 kV/cm, while the undoped BST ceramics have a higher leakage current density of 2.79×10^{-7} A/cm at the same applied electric field. The decrease in the leakage current density of the BST0510 ceramics could be explained as follows. Just as in the acceptors doping of BST ceramics [10,20–22], the effect of Mn/Y-codoping on the leakage current density has been attributed to the Mn and Y behavior as electron acceptor-type dopants, which reduces the net charge in the BST. Moreover, the decreased leakage current also is dependent on the bulk density of these BST ceramics, as shown in Fig. 1.

4. Conclusions

This investigation demonstrates that Mn/Y codoping has a strong influence on the microstructure and electrical properties of BST ceramics. We have achieved improved dielectric properties of 0.5 mol% Mn/1.0 mol% Y-codoped BST ceramics compared with that of undoped BST ceramics. The measured values of remanent polarization ($2P_r$), coercive field ($2E_c$), and leakage current of $Ba_{0.67}Sr_{0.33}TiO_3$ ceramics codoped with 0.5 mol% Mn and 1.0 mol Y are 15.327 μC/cm^2, 3.456 kV/cm, and 1.23×10^{-7} A/cm^2 at $E = 10$ kV/cm, respectively. The dielectric loss of 0.5 mol% Mn/1.0 mol% Y-codoped BST ceramics is the lowest among all BST ceramics, and its steep dielectric constant peak benefits to a pyroelectric application.

Acknowledgements

The work was supported by the Natural Science Foundation of China (Grant Nos. U0837605 and 60771016). The authors would like to thank Dr. Chaoliang Zhang for the SEM analysis and Mr. Yong Jin for the XRD data collection.

References

[1] H.J. Noh, S.G. Lee, S.P. Nam, Y.H. Lee, Pyroelectric properties of arrayed BaTiO3 system thick film for uncooled IR detector, Materials Research Bulletin 45 (3) (2010) 339–342.
[2] C. Sun Gyu, H. Tae-Jung, Y. Byoung-Gon, J. Seung Pil, O. Kwon, P. Hyung-Ho, Improvement of uncooled infrared imaging detector by using mesoporous silica as a thermal isolation layer, Ceramics International 34 (4) (2008) 833–836836.
[3] T. Kim, N.V. Gaponenko, Sol–gel synthesis of barium-strontium titanate in porous anodic alumina for uncooled IR detector, in: International Workshop on Terahertz and mid Infrared Radiation: Basic Research and Practical Applications, 2009.
[4] M. Noble, P. Bemasconi, A. Francomacaro, H. Eaton, B. Carkhuff, P. Foukal, Barium strontium titanate (BST) pyroelectric detector for bolometric solar imaging, Infrared Systems and Photoelectronic Technology 7055 (2008) 550.
[5] M.W. Cole, E. Ngo, S. Hirsch, M.B. Okatan, S.P. Alpay, Dielectric properties of MgO-doped compositionally graded multilayer barium strontium titanate films, Applied Physics Letters 92 (7) (2008).
[6] L.C. Costa, A. Aoujgal, M.P.F. Graca, N. Hadik, M.E. Achour, A. Tachafine, J.C. Carru, A. Oueriagli, A. Outzourit, Microwave dielectric properties of the system $Ba_{1-x}Sr_xTiO_3$, Physica B: Condensed Matter 405 (17) (2010) 3741–3744.
[6] L.C. Costa, A. Aoujgal, M.P.F. Graca, N. Hadik, M.E. Achour, A. Tachafine, J.C. Carru, A. Oueriagli, A. Outzourit, Microwave dielectric properties of the system $Ba_{1-x}Sr_xTiO_3$, Physica B 405 (2010) 3741–3744.
[8] G. Liu, H.L. Guo, P. Yu, D.Q. Xiao, J.G. Zhu, Study on intrinsic pyroelectric property of Mn doped BST ceramics, Function Materials 6 (2010) 1053–1056.
[9] D. Makovec, Z. Samardzija, M. Drofenik, Solid solubility of holmium, yttrium, and dysprosium in $BaTiO_3$, Journal of the American Ceramic Society 87 (7) (2004) 1324–1329.
[10] R.V. Wang, P.C. McIntyre, J.D. Baniecki, K. Nomura, T. Shioga, K. Kurihara, M. Ishii, Effect of Y doping and composition-dependent elastic strain on the electrical properties of (Ba,Sr)TiO_3 thin films deposited at 520 °C, Applied Physics Letters 87 (19) (2005).
[11] A. Ioachim, M.I. Toacsan, M.G. Banciu, L. Nedelcu, A. Dutu, S. Antohe, C. Berbecaru, L. Georgescu, G. Stoica, H.V. Alexandru, Transitions of barium strontium titanate ferroelectric ceramics for different strontium content, Thin Solid Films 515 (16) (2007) 6289–6293.
[12] T. Hu, T.J. Price, D.M. Iddles, A. Uusimaki, H. Jantunen, The effect of Mn on the microstructure and properties of $BaSrTiO_3$ with B_2O_3-Li_2CO_3, Journal of the European Ceramic Society 25 (12) (2005) 2531–2535.
[13] C.V. Weiss, M.B. Okatan, S.P. Alpay, M.W. Cole, E. Ngo, R.C. Toonen, Compositionally graded ferroelectric multilayers for frequency agile tunable devices, Journal of Materials Science 44 (19) (2009) 5364–5374.
[14] M. Noda, K. Inoue, H. Zhu, H. Xu, T. Mukaigawa, M. Okuyama, A chopperless-operated dielectric bolometer mode of infrared image sensor with ferroelectric BST film using improved operation, in: Proceedings of the 2001 12th IEEE International Symposium on Applications of Ferroelectrics, 2001.
[15] S.J. Liu, C.Y. Xu, X.B. Zeng, B.F. Zhao, Dielectric properties of $(Ba_{0.67}Sr_{0.33})TiO_3$ thin film for uncooled infrared focal plane arrays, European Physical Journal: Applied Physics 19 (3) (2002) 181–183.
[16] C.G. Wu, W.L. Zhang, Y.R. Li, X.Z. Liu, J. Zhu, B.W. Tao, High pyroelectric $Ba_{0.65}Sr_{0.35}TiO_3$ thin films with $Ba_{0.65}Sr_{0.35}RuO_3$ seeding-layer for monolithic ferroelectric bolometer, Infrared Physics and Technology 48 (3) (2006) 187–191.

[17] M. Noda, H. Zhu, H.P. Xu, T. Mukaigawa, K. Hashimoto, T. Kiyomoto, R. Kubo, H. Tanaka, T. Usuki, M. Okuyama, A new dielectric bolometer mode of detector pixel for uncooled infrared image sensor with ferroelectric BST thin film prepared by metal-organic decomposition, Integrated Ferroelectrics 35 (1–4) (2001) 1761–1769.

[18] M. Noda, K. Hashimoto, R. Kubo, H. Tanaka, T. Mukaigawa, H.P. Xu, M. Okuyama, A new type of dielectric bolometer mode of detector pixel using ferroelectric thin film capacitors for infrared image sensor, Sensors and Actuators A: Physical 77 (1) (1999) 39–44.

[19] M. Noda, T. Mukaigawa, K. Hashimoto, T. Kiyomoto, H.P. Xu, R. Kubo, H. Tanaka, T. Usuki, M. Okuyama, A simple detector pixel of dielectric bolometer mode and its device structure for uncooled IR image sensor, Infrared Technology and Applications X 3698 (1999) 565–573.

[20] S.Y. Wang, B.L. Cheng, C. Wang, S.A.T. Redfern, S.Y. Dai, K.J. Jin, H.B. Lu, Y.L. Zhou, Z.H. Chen, G.Z. Yang, Influence of Ce doping on leakage current in $Ba_{0.5}Sr_{0.5}TiO_3$ films, Journal of Physics Part D: Applied Physics 38 (13) (2005) 2253–2257.

[21] J.K. Kim, S.S. Kim, W.J. Kim, T.G. Ha, I.S. Kim, J.S. Song, R. Guo, A.S. Bhalla, Improved ferroelectric properties of Cr-doped $Ba_{0.7}Sr_{0.3}TiO_3$ thin films prepared by wet chemical deposition, Materials Letters 60 (19) (2006) 2322–2325.

[22] M. Jain, S.B. Majumder, R.S. Katiyar, F.A. Miranda, F.W. Van Keuls, Improvement in electrical characteristics of graded manganese doped barium strontium titanate thin films, Applied Physics Letters 82 (12) (2003) 1911–1913.